Polymer Science, Ser. A, Vol. 45, No. 4, 2003, pp. 386–393. Translated from Vysokomolekulyarnye Soedineniya, Ser. A, Vol. 45, No. 4, 2003, pp. 631–640.
Original Russian Text Copyright © 2003 by Trofimchuk, Nikonorova, Bakeev, Zezin, Lebedeva, Volynskii.
English Translation Copyright © 2003 by MAIK "Nauka/Interperiodica" (Russia).

The Crystallization Behavior of Silver Chloride in Different Porous Polymers Prepared Using the Solvent Crazing Technique[1]

E. S. Trofimchuk*[2], N. I. Nikonorova[3], N. F. Bakeev*, S. B. Zezin*, O. V. Lebedeva, and A. L. Volynskii***

** Faculty of Chemistry, Moscow State University, Leninskie gory, Moscow, 119992 Russia*

*** Institute of Synthetic Polymeric Materials, Russian Academy of Sciences, Profsoyuznaya ul. 70, Moscow, 117393 Russia*

Received May 23, 2002;
Revised Manuscript Received December 2, 2002

Abstract—The formation and structure of the silver chloride crystal phase produced in an exchange reaction in solvent-crazed porous polymer matrices with initially different physical states were studied. The effects of the nature and structure of a porous matrix on the formation rate of the new phase, its dispersion, and the aggregation type of silver chloride particles were considered. A mechanism was proposed for the crystallization of silver chloride in porous media.

INTRODUCTION

The preparation and stabilization of polymer–inorganic hybrid materials with nanoscale dispersion remains a topical problem despite the great variety of available approaches to the design of such materials [1, 2].

One of the most important and promising processes for the manufacture of these composites is the synthesis of particles of a new phase in porous polymeric matrices prepared using the technique of crazing in liquid media [3]. Crazed polymers have a specific interpenetrating fibrillar–porous structure comprising an evolutionary system of fibrils and nanosized pores, which can impart specific features to the processes of crystallization and formation of a new phase in the pores. Earlier [4–8], we studied some specifics of the crystallization of nickel particles in similar porous polymeric matrices and proposed certain empirical approaches for the prediction of the structural design of metal–polymer composites. However, the reduction of nickel is an exothermic and autocatalytic process. Therefore, it seemed interesting to study the proceeding, in crazed polymers, of chemical reactions of other types affording a low-molecular-mass substance as an individual phase. For this purpose, we studied the formation and structure of an AgCl phase precipitated upon the relevant reaction without releasing by-products. Earlier, we studied the formation of AgCl nanoparticles in small closed volumes, such as microemulsions [9, 10], an amorphous silicon dioxide matrix [11], and porous polymers [12, 13].

In this work, we studied the reaction kinetics, structure, and formation processes for aggregates of the new AgCl phase in two porous polymeric matrices of PET and PP which differed in the physical state of the starting matrices. It was also hoped that the study would provide new information on the porous structure of polymers obtained using the solvent crazing technique.

EXPERIMENTAL

Starting porous polymeric materials were prepared from commercial films of semicrystalline isotactic PP ($M_w = 3 \times 10^5$, a thickness of 130 μm, $T_g = -8°C$) and amorphous PET ($M_w = 3 \times 10^5$, a thickness of 110 μm, $T_g = 70°C$) by tensile drawing in isopropanol to 50, 250, and 400% at a speed of 5 mm/min. The craze generation and development of the porous structure followed the classical solvent crazing mechanism [3]. The effective bulk porosity was determined according to a standard procedure [14] by measuring the increment of volume of a specimen during its deformation in an adsorption-active medium (AAM).

Silver chloride particles were obtained using the exchange reaction between silver nitrate ($AgNO_3$) and sodium chloride (NaCl). Aqueous–alcoholic (4 : 1) solutions of reactants with a salt concentration of 0.15 mol/l were used. The reactants were introduced into a polymeric matrix using the countercurrent diffusion technique. Prior to this, preliminarily prepared polymeric membranes were held in a water : isopro-

[1] This work was supported by the Russian Foundation for Basic Research, project no. 01-03-32596a.
[2] E-mail: elena_trofimchuk @mail.ru
[3] E-mail: nni@genebee.msu.ru

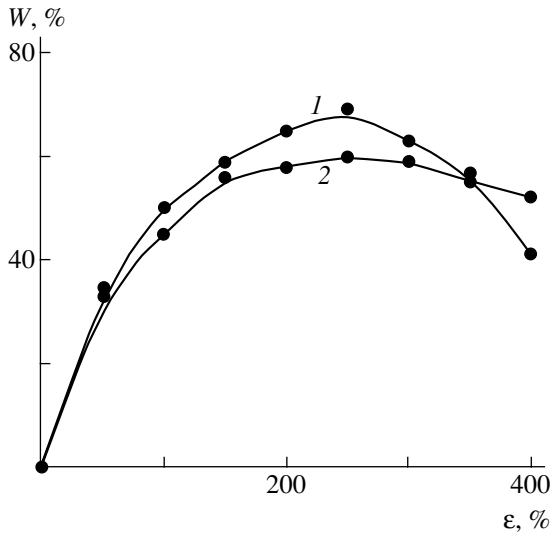

Fig. 1. The effective bulk porosity as a function of the (*1*) PET and (*2*) PP deformation ratio in isopropanol.

panol mixture (4 : 1) for a day to replace isopropanol by a medium resembling the reaction mixture in composition. The reaction time varied from 5 min to 1 h. To remove soluble impurities, the AgCl-containing films were washed with distilled water and dried in a strained state at 60°C to constant mass. To avoid the reduction of silver to the metal state upon exposure to light, all manipulations (reacting, washing, and drying) were conducted in the dark.

The mass of AgCl produced in porous polymer films was determined using a gravimetric procedure ($q = \frac{m_{AgCl}}{m_p}$, where m_p is the mass of the initial porous polymeric matrix). The relative error in determination of AgCl was 10–15%.

The X-ray diffraction analysis of specimens was performed with a DRON-3M instrument using CuK_α ($\lambda = 1.54$ Å) radiation. Reflections were assigned using the structure database JCPDS–ICDD [15]. The average crystallite size B was determined using a graphical method [16] allowing simultaneous determination of the degree of crystal-lattice imperfection. For cubic AgCl crystals, the half-width at half-maximum β was found for all diffraction lines and the curve of $\frac{1}{B^2} = \left(\frac{\beta\cos\theta}{\lambda}\right)^2$ was plotted against $\left(\frac{\sin\theta}{\lambda}\right)^2$. The quantity β is defined as $\sqrt{\beta_{exp}^2 - \beta_0^2}$, where β_{exp} and β_0 are the experimental and instrumental half-widths of diffraction maximums, respectively, and θ is the Bragg reflection angle at the maximum intensity. The value of $1/B^2$ corresponding to $\left(\frac{\sin\theta}{\lambda}\right)^2 = 0$ gave the true magnitude of $1/B^2$, and the slope of the straight line gave the deviation of lattice parameters from average values $\frac{\Delta a}{a} = \frac{\beta}{2\tan\theta}$, where a is the spacing of the cubic lattice.

The morphology of the composites obtained was examined with a Hitachi S-520 scanning electron microscope. Samples were prepared using the procedure of brittle fracture in liquid nitrogen and decoration with a platinum–palladium alloy.

RESULTS AND DISCUSSION

Characterization and Structure of Original Matrices

The porous polymer structure obtained as result of solvent crazing is a labile, highly dispersed system characterized by certain average effective pore and fibril sizes and bulk porosity. These parameters depend on several factors: the AAM nature, polymer deforma-

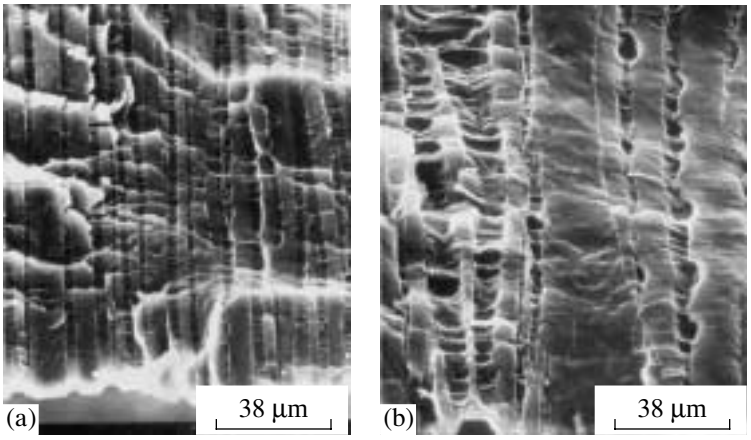

Fig. 2. Microphotographs of initial porous (a) PET and (b) PP matrices; $\varepsilon = 50\%$.

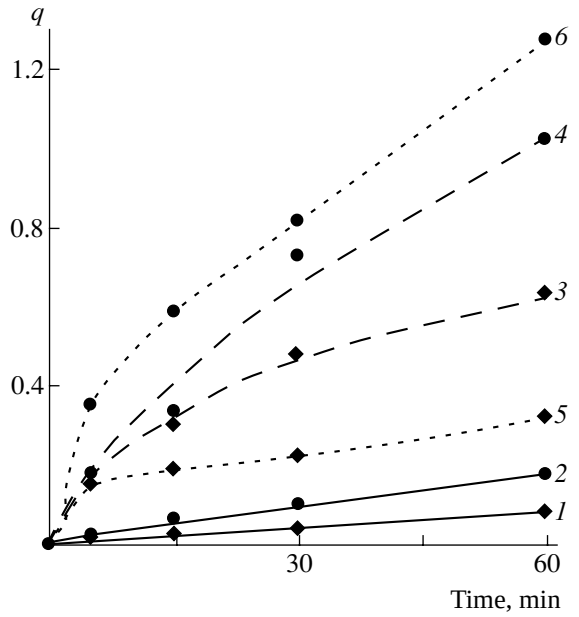

Fig. 3. Buildup curves for AgCl particles depending on the reaction time in different porous (*1*, *3*, *5*) PET and (*2*, *4*, *6*) PP matrices deformed in isopropanol to (*1*, *2*) 50, (*3*, *4*) 250, and (*5*, *6*) 400%.

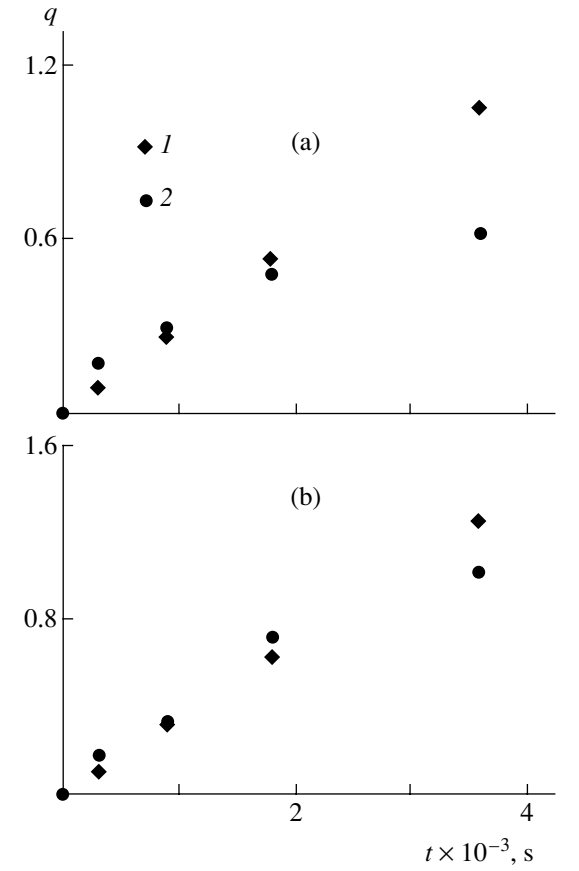

Fig. 4. (*1*) Theoretical and (*2*) experimentally measured amounts of AgCl plotted against the reaction time in porous (a) PET and (b) PP matrices; ε = 250%.

tion ratio, temperature, etc. The effective bulk porosity W is one of the basic characteristics of porous polymeric matrices prepared through solvent crazing. In the present work, W was measured only by varying the polymer deformation ratio ε; other deformation and AAM parameters remained unchanged. Figure 1 shows $W(\varepsilon)$ plots for PET and PP upon their tensile drawing in an isopropanol medium. It is seen that W is a nonmonotonous function of ε, which is characteristic of polymers whose porous structure develops via the classical solvent crazing mechanism [3]. Various matrices with identical deformation ratios have close W values. The mean pore size for PET, as determined using the conventional procedure [14], is 2–15 nm [17]; for PP, this quantity ranges within 7–10 nm [18].

The typical morphology of porous polymer matrices prepared through the classical solvent crazing mechanism is shown in Fig. 2. The structure of the polymer elongated to a deformation ratio of 50% is a system of interpenetrating pores separated by bulk regions of unoriented polymer (Fig. 2). As the deformation ratio increases to 250%, the proportion of the crazed material increases through growth and widening of the crazes formed. Such a polymer has a maximum porosity of 60–65%, and the dimensions of the crazed and bulk regions are comparable. At high deformation ratios (400%), the porous structure starts to collapse; this process is accompanied by significant structural rearrangements [3]. Thus, for each type of polymer, porous matrices with three deformation ratios of 50, 250, and 400% having different parameters of their porous structure and different morphologies were used.

The Kinetics of Silver Chloride Formation in Porous Polymer Matrices

Figure 3 shows the AgCl gain q plotted against the time t of exchange reaction in different polymeric matrices. The $q(t)$ plots for PET and PP with ε = 50% (curves *1*, *2*) are linear. For the porous matrices deformed by 250 and 400%, the AgCl buildup has the highest rate at the initial product formation steps. Further, the buildup rate gradually decreases. The analysis of kinetic curves for polymeric matrices of the same nature shows that the amount of substance introduced varies symbatically with porosity. This means that the bulk porosity is a factor determining the product buildup process. Note that the PET matrices are characterized by a faster decrease in the AgCl buildup rate with reaction time as compared to the PP matrices and some $q(t)$ plots (curves *3*, *5*) tend to reach a plateau. In this case, the amount of AgCl produced in PP for 60 min is greater than in the PET matrices having the same bulk porosity.

Thus, there are substantial differences in the AgCl formation kinetics in crazed porous PET and PP matrices despite close values for the effective bulk porosity and identical diffusion rates of low-molecular-mass reactants. This may be due to the difference in the mor-

Comparative structural–morphological characteristics of porous PET and PP matrices containing AgCl particles

ε, %	*t*, min	Degree of filling, vol %	*B*, nm	Δ*a*/*a*, %	Characterization of AgCl localization sites	*H*, μm	D_{agg}, μm
				PET			
50	5	–	–	–	–	–	–
	15	0.6	55	0.4	Single aggregates	–	up to 1
	30	1.8	43	0.6	Single rodlike aggregates	10	1–5
250	5	0.7	80	0.4	Single aggregates	2.5	4
	15	3.2	24	0.6	The same	8	5–8
	30	5.7	36	0.6	The same	7	5–10
400	5	4.3	28	0.6	–	–	–
	15	6.3	19	0.6	Discontinuous layer	15	0.1–0.2
	30	7.6	18	0.6	Virtually continuous layer	15	0.1–0.2
				PP			
50	5	1.4	90	0.3	Loose discontinuous layer	30	0.3–0.5
	15	2.7	75	0.3	Discontinuous layer	35	0.3–0.5
	30	3.9	50	0.4	The same	40	0.3–0.5
250	5	2.2	80	0.3	Loose discontinuous layer	25	up to 0.2
	15	6.5	75	0.5	Discontinuous layer	25	0.2–0.3
	30	6.9	90	0.3	Continuous layer	25	0.2–0.3
400	5	5.0	65	0.4	Discontinuous layer	8	0.1
	15	10.8	80	0.3	The same	10	0.1–0.2
	30	12.2	60	0.4	Continuous layer	15	0.1–0.3

phologies of crazes and the different labilities of the porous structure of PET and PP matrices.

The theoretical $q(t)$ plot for porous PET and PP (ε = 250%) was calculated on the basis of the theory of diffusion-controlled processes. The overall process was assumed to occur in two steps in this case [6–8]. The first step is the diffusion of reactants inside the polymeric matrix to the reaction front (the slow, rate-limiting step of the overall process), and the second step is a chemical reaction with product formation and precipitation of a new phase (fast step). We based our calculations on the following assumptions: a porous polymeric membrane is a system of through cylindrical pores arranged perpendicular to the polymer film surface and separated by the bulk polymer; there is a partition coefficient K of reactants distributed between the initial solution and the membrane, i.e., c_0' (in pore) = Kc_0 (in solution); the diffusion of ions along a pore to the reaction front is one-dimensional and is described by Fick's first law; the reactants arrive at the reaction front instantaneously and quantitatively enter into the exchange reaction.

The amount of AgCl (m_{AgCl} (g)) formed for a time t can be determined [7, 8] using the expression

$$m_{AgCl} = \frac{DS_{pores}Kc_0}{l}M_{AgCl}t. \quad (1)$$

Here, D is the diffusion coefficient of $AgNO_3$, K is the $AgNO_3$ partition coefficient between the reactant solution and polymeric membrane, S_{pores} is the area of pores on the polymer film surface ($S_{pores} = \frac{W}{1-W}\frac{V_p}{h_p} = \frac{W}{1-W}\frac{m_p}{\rho_p h_p}$, where W is the effective bulk porosity of the polymeric matrix and V_p, m_p, ρ_p, and h_p are the polymer volume, mass, density, and thickness, respectively), c_0 is the initial concentration of the $AgNO_3$ solution, l is the distance from the membrane surface to the reaction front, and M_{AgCl} is the molar mass of AgCl. After appropriate substitutions, we obtain the following calculation formula:

$$q = \frac{DKc_0M_{AgCl}W}{l\rho_p(1-W)h_p}t.$$

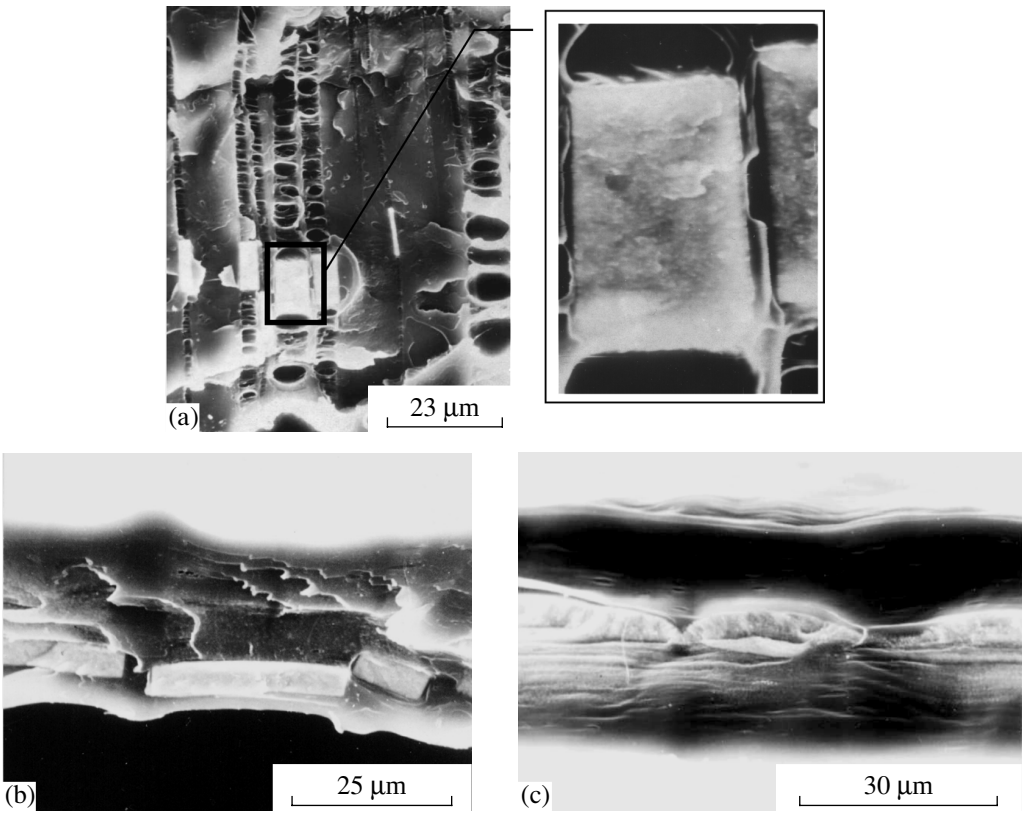

Fig. 5. Microphotographs of AgCl-containing PET specimens at ε = (a) 50, (b) 250, and (c) 400%. Precipitation reaction times of (a) 30 and (b, c) 15 min.

The quantities K and D in porous crazed polymeric matrices were experimentally determined using a procedure described in [19]. It turned out that the partition constant in the PET (ε = 250%) and PP (ε = 250%) matrices is equal to 0.204 and 0.352, respectively, and the diffusion coefficient in PET (ε = 250%) and PP (ε = 250%) is equal to $(2.5 \pm 0.5) \times 10^{-10}$ and $(1.6 \pm 0.5) \times 10^{-10}$ m^2/s, respectively. Note that the diffusion coefficient of $AgNO_3$ in an infinitely dilute solution (1.76×10^{-9} m^2/s) is ten times higher than that in porous polymers. This difference may be associated with the fact that the actual diffusion path of a substance in a porous polymeric matrix is significantly greater than its thickness because of the presence of craze wall–connecting fibrils and pore branching.

The distance to the reaction front l was determined from the scanning electron microscopy data, since it coincides with the distance from the film surface to the dense portion of the AgCl layer. It was found that l = 60 μm.

Calculated and experimental $q(t)$ curves obtained for different polymeric matrices are shown in Fig. 4. It is seen that they coincide well at the initial AgCl formation stages. At later stages, there are significant deviations of the theoretical results from the experimental results, which is due to the gradual slowing down of the formation of the new phase. Note that the discrepancy between theory and experiment for the rigid PET matrix (under the given experimental conditions, the polymer occurs in the glassy state) is more significant than that for PP. This difference seems to result from a decrease in the matrix permeability to reactants by virtue of the decrease in the bulk porosity of the polymer because of precipitation of AgCl in its pores. Indeed, as shown for porous PP matrices in [18], the addition of 50% nickel almost halved their permeability.

To summarize, the calculated and experimental data showed that the kinetics of AgCl buildup in porous polymeric matrices, in which the diffusion of reactants to the reaction front is a rate-limiting step, are complex in character. At the initial stage, the rate of the process is determined only by the magnitude of bulk porosity. Therefore, the precipitation reaction proceeds with identical rates in chemically different matrices with close values of bulk porosity. Marked differences for the matrices in question (slowing down and even saturation) are observed at later reaction stages, which are determined by the physical state of the matrix and the lability of the porous structure of the polymers. If this assumption is true, the polymer nature will probably affect both the size of crystallites during their formation

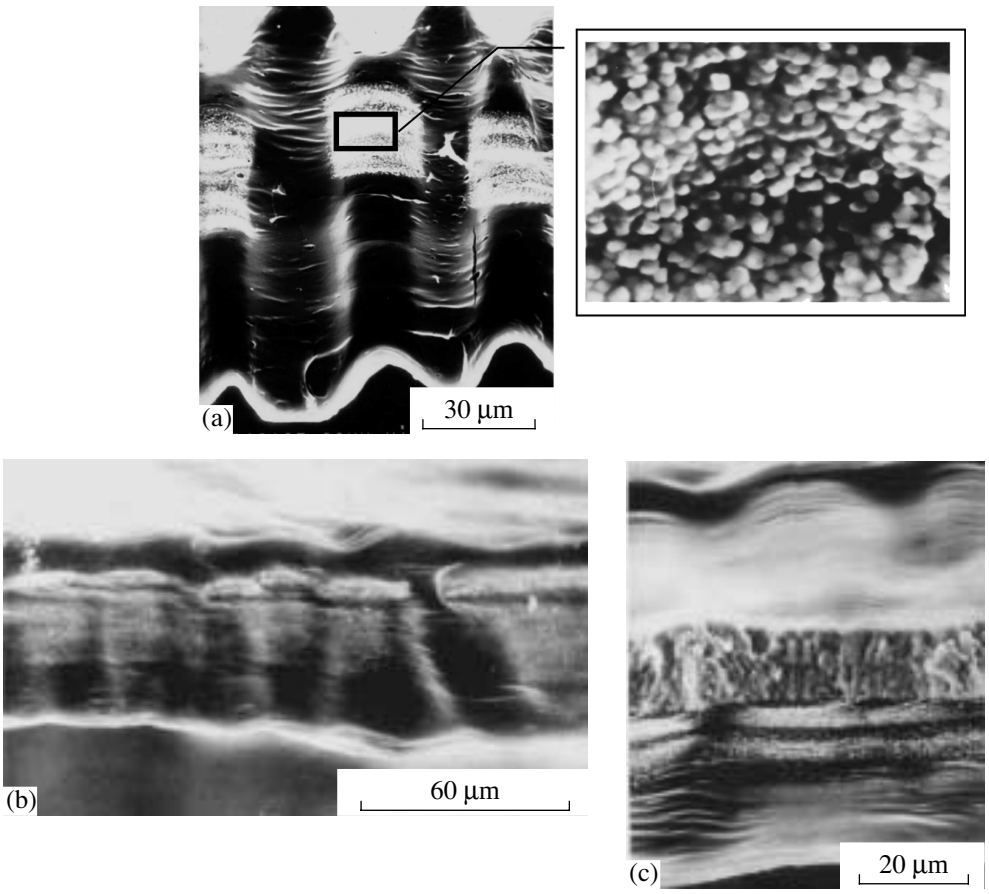

Fig. 6. Microphotographs of AgCl-containing PP specimens at ε = 250% and the precipitation reaction time of (a) 5, (b) 15, and (c) 60 min.

and the manner of their distribution in the porous matrix.

Structural–Morphological Study of Silver Chloride Crystallization in Porous Matrices

Using the X-ray diffraction technique, we found that the AgCl crystal phase is formed upon the exchange reaction in all of the polymeric matrices examined. Interplanar spacings referring to the most intense reflections were calculated from diffractograms to give 2.7, 3.20, and 1.96 Å for the planes {200} (d_{theor} = 2.774), {111} (d_{theor} = 3.203), and {220} (d_{theor} = 1.962), respectively.

The table lists the values of B and $\Delta a/a$ for AgCl crystallites produced in porous polymer matrices. The diameter of AgCl crystallites formed in a macroscopic volume under the same conditions is greater than 120 nm. According to the data given in the table, crystallites with a diameter of 70–90 nm are formed at the initial reaction stage (t = 5 min) in all porous PP and PET matrices (ε = 250%). In PET with ε = 400%, the crystallite diameter is threefold smaller and equal to 28 nm. By this time, no AgCl phase could be detected in PET with ε = 50% because of its small amount (<2 wt %). The average crystallite size at later formation stages of the new phase depends on both the nature of the porous matrix and the parameters of the porous structure. The average diameter of AgCl crystallites obtained in PET for 30 min is reduced to 20–40 nm. In PP, this quantity remains virtually time-invariant (60–80 nm). The degree of crystallite imperfection turned out to be insignificant, it is slightly affected by the nature of the porous matrix and almost does not vary as the amount of AgCl increases. For example, the deviation of the AgCl lattice parameter $\Delta a/a$ from the average value is (0.5–0.6) ± 0.1% and (0.3–0.4) ± 0.1% in the PET and PP matrices, respectively.

Note that the diameter of AgCl crystallites produced is substantially larger than the average pore diameter in the polymeric matrix. It may be assumed that in a crazed polymer a pore size distribution is formed and there are large pores. However, a more plausible mechanism for the formation of large crystals consists in that the fibrillar–porous structure undergoes evolution during phase separation and the AgCl crystals formed move the flexible polymer fibrils connecting craze walls apart [12]. The crystal growth seems to proceed

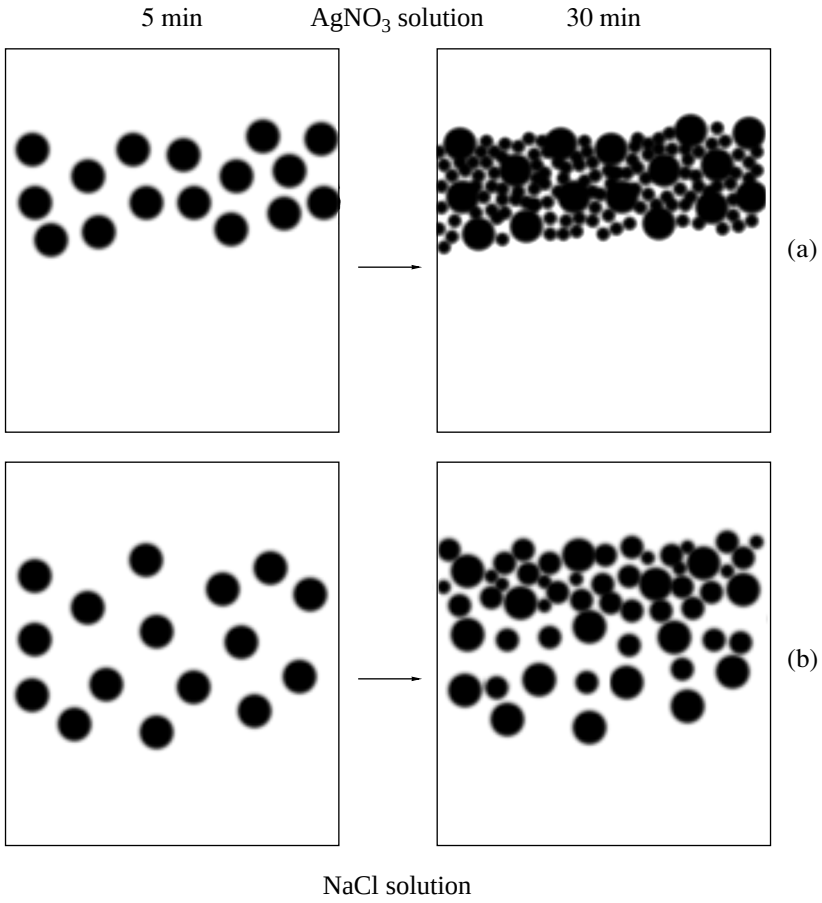

Fig. 7. Schematic of the formation of a new AgCl phase in porous (a) PET and (b) PP matrices. The circles represent AgCl particles.

until the process of moving fibrils apart becomes impossible without their failure. Gradually, fibrils become less compliant because of the precipitation of AgCl particles on them; thus, a decrease in the mean crystallite diameter takes place. The porous PET structure is more rigid and the mobility of fibrils is lower than in PP. This difference seems to be responsible for the smaller average diameter of AgCl crystallites produced in PET.

The morphology of obtained samples was also examined with an electron microscope. Figures 5 and 6 show the microphotographs of different porous polymer matrices containing the AgCl phase. The comparison of the structures of initial polymeric matrices (Fig. 2a) with those containing the AgCl phase (Fig. 5a) shows that the composite structure is determined by the structure of the porous matrix when the reactants are introduced by means of countercurrent diffusion.

In the PET matrices, the AgCl phase forms a sufficiently dense layer (reaction time of 30 min) composed of rodlike aggregates spatially separated by unoriented-polymer regions (Figs. 5a, 5b). The height of the aggregates is the same as the layer thickness H and equals 7–10 μm. As the craze width increases, the length of AgCl aggregates increases from ~1–5 μm in PET with ε = 50% to 10–15 μm in PET with ε = 250%. On the basis of the results of our earlier study [12] and the X-ray diffraction and microscopy data obtained in this work, we may state that a dense rodlike aggregate is a system of nanocrystals and polymer fibrils. For example, the average AgCl crystallite size in PET (ε = 50%) is equal to 43 nm and the linear dimension of the rod aggregate is much greater than 1 μm.

In PET with ε = 400% (Fig. 5c), AgCl forms a virtually continuous broad layer with nonuniform density. The layer is composed of individual spherical and cubic aggregates with a dimension of D_{agg} = 100–300 nm; the looser portion is composed of smaller aggregates. This morphology is probably due to the specific features of the porous structure of the polymeric matrix at high deformation ratios [3]. Such a polymer consists of oriented aggregates of fibrils with microvoids in between.

The steps of layer formation in a porous PP matrix are shown in Fig. 6. First, a loose discontinuous layer is formed in the polymer from rather extended regions containing spherical and cubic AgCl particles of 200–300 nm in diameter, which are probably crystallite aggregates (Fig. 6a). Upon further accumulation of

AgCl in polymer pores, these regions gradually expand (Fig. 6b), forming a continuous layer (Fig. 6c). Dense and loose (composed of smaller aggregates) portions can be distinguished in the latter layer. The thickness of the layer (table) depends on the structure of the initial porous PP matrix and equals 15–40 μm.

CONCLUSIONS

The analysis of the kinetic, structural, and morphological data allows the formation of the AgCl in porous polymer media to be represented as follows (Fig. 7). In the initial steps of the separation of the new phase, relatively large AgCl crystallites are formed. Further buildup of the product involves the release of new crystallites, with their average size gradually decreasing. This is distinctly seen in the porous matrices based on PET. The growth of crystallites is due to the moving apart of flexible fibrils connecting craze walls. The crystals formed gather into larger particles, involving polymer fibrils into the aggregation process.

Silver chloride aggregates gradually form a layer in polymeric matrices, which is detected using the technique of electron microscopy. The layer density and the presence of polymer interlayers in this layer depend on the nature of the polymeric matrix, the parameters of porous structure, and the size of the AgCl crystallites. In the case of PET (Fig. 7a), the mean crystallite diameter noticeably decreases in the course of crystallization: smaller crystallites fill the space between initially formed large crystallites, forming very dense rodlike aggregates. Note that such a layer is virtually impermeable to reactants and the rate of AgCl precipitation reaction rapidly decreases with time (Fig. 3, curve *3*). In PET, filling with the new phase proceeds until a bulk porosity of 6.0–7.5% of the original matrix is reached. In the PP matrix (Fig. 7b), the dimensions of crystallites and their aggregates slightly vary with time and the particles form a relatively loose nonuniform layer. Such a layer remains permeable to the reactants for a long while; therefore, the AgCl buildup process in the PP matrix takes a longer time (Fig. 3, curves *4*, *6*) and the filler volume content may reach 12% of the bulk porosity of the original matrix.

REFERENCES

1. Ellsworth, M.W. and Gin, D.L., *Polym. News*, 1999, vol. 24, p. 331.
2. Pomogailo, A.D., Rozenberg, A.S., and Uflyand, I.E., *Nanochastitsy metallov v polimerakh* (Metal Nanoparticles in Polymers), Moscow: Khimiya, 2000.
3. Volynskii, A.L. and Bakeev, N.F., *Vysokodispersnoe orientirovannoe sostoyanie polimerov* (Highly Dispersed Oriented State of Polymers), Moscow: Khimiya, 1984.
4. Stakhanova, S.V., Nikonorova, N.I., Zanegin, V.D., Lukovkin, G.M., Volynskii, A.L., and Bakeev, N.F., *Polymer Science*, 1992, vol. 34, no. 2, p. 175.
5. Stakhanova, S.V., Trofimchuk, E.S., Nikonorova, N.I., Rebrov, A.V., Ozerin, A.N., Volynskii, A.L., and Bakeev, N.F., *Polymer Science, Ser. A*, 1997, vol. 39, no. 2, p. 229.
6. Stakhanova, S.V., Nikonorova, N.I., Volynskii, A.L., and Bakeev, N.F., *Polymer Science, Ser. A*, 1997, vol. 39, no. 2, p. 224.
7. Nikonorova, N.I., Stakhanova, S.V., Volynskii, A.L., and Bakeev, N.F., *Polymer Science, Ser. A*, 1997, vol. 39, no. 8, p. 882.
8. Nikonorova, N.I., Trofimchuk, E.S., Elkin, P.G., Belova, N.E., Fanchenko, S.S., Volynskii, A.L., and Bakeev, N.F., *Polymer Science, Ser. A*, 2002, vol. 44, no. 7, p. 744.
9. Bagwe, R.P. and Khilar, K.C., *Langmuir*, 1997, vol. 13, no. 24, p. 6432.
10. Bagwe, R.P. and Khilar, K.C., *Langmuir*, 2000, vol. 16, no. 3, p. 905.
11. Zayat, M., Einot, D., and Reisfeld, R., *J. Sol–Gel Sci. Technol.*, 1997, vol. 10, p. 67.
12. Volynskii, A.L., Yarysheva, L.M., Arzhakova, O.V., and Bakeev, N.F., *Vysokomol. Soedin., Ser. A*, 1991, vol. 33, no. 2, p. 418.
13. Volynskii, A.L., Grokhovskaya, T.E., Shitov, N.A., and Bakeev, N.F., *Vysokomol. Soedin., Ser. B*, 1980, vol. 22, no. 7, p. 483.
14. Arzhakova, O.V., Yarysheva, L.M., Gal'perina, I.B., Volynskii, A.L., and Bakeev, N.F., *Vysokomol. Soedin., Ser. B*, 1989, vol. 31, no. 12, p. 887.
15. *JCPDS-ICDD Database, File 31-1238*, 1995.
16. Kovba, L.M. and Trunov, V.K., *Rentgenofazovyi analiz* (X-ray Diffraction Analysis), Moscow: Mosk. Gos. Univ., 1969, p. 132.
17. Volynskii, A.L., Kozlova, O.V., and Bakeev, N.F., *Vysokomol. Soedin., Ser. A*, 1985, vol. 27, no. 12, p. 2169.
18. Stakhanova, S.V., *Cand. Sci. (Chem.) Dissertation*, Moscow: Moscow State Univ., 1996.
19. Trofimchuk, E.S., Nikonorova, N.I., Bakeev, N.F., Zezin, S.B., Lebedeva, O.V., and Volynskii, A.L., *Zh. Obshch. Khim.* (in press).